Suggestions for benchmark scenarios for MSSM Higgs boson searches at hadron colliders

M. Carena[1,a], S. Heinemeyer[2,b], C.E.M. Wagner[3,4,c], G. Weiglein[5,d]

[1] Theoretical Physics Department, Fermilab National Accelerator Laboratory, Batavia, IL 60510-0500, USA
[2] Institut für theoretische Elementarteilchenphysik, LMU München, Theresienstr. 37, 80333 München, Germany
[3] HEP Division, Argonne National Laboratory, 9700 Cass Ave., Argonne, IL 60439, USA
[4] Enrico Fermi Institute, University of Chicago, 5640 Ellis Ave., Chicago, IL 60637, USA
[5] Institute for Particle Physics Phenomenology, University of Durham, Durham DH1 3LE, UK

Abstract. The Higgs boson search has shifted from LEP2 to the Tevatron and will subsequently move to the LHC. Due to the different initial states, the Higgs production and decay channels relevant for Higgs boson searches are different at hadron colliders compared to LEP2. We suggest new benchmark scenarios for the MSSM Higgs boson search at hadron colliders that exemplify the phenomenology of different parts of the MSSM parameter space. Besides the m_h^{max} scenario and the no-mixing scenario used in the LEP2 Higgs boson searches, we propose two new scenarios. In one scenario the main production channel at the LHC, $gg \to h$, is suppressed over a wide part of the M_A–$\tan\beta$-plane. In the other scenario, important Higgs decay channels at the Tevatron and at the LHC, $h \to b\bar{b}$ and $h \to \tau^+\tau^-$, can be suppressed. All scenarios fulfill the LEP2 constraints for nearly the whole M_A–$\tan\beta$-plane.

1 Introduction and theoretical basis

Within the MSSM the masses of the $\mathcal{CP}$-even neutral Higgs bosons are calculable in terms of the other MSSM parameters. The lightest Higgs boson has been of particular interest, since its mass, m_h, is bounded from above according to $m_h \leq M_Z$ at the tree level. The radiative corrections at one-loop order [1] have been supplemented in the last years with the leading two-loop corrections, performed by renormalization group (RG) methods [2], by renormalization group improvement of the one-loop effective potential calculation [3,4], by two-loop effective potential calculations [5,6], and in the Feynman-diagrammatic (FD) approach [7,8]. These calculations predict an upper bound for m_h of about $m_h \lesssim 135\,\mathrm{GeV}$ [1].

After the termination of LEP, the Higgs boson search has now shifted to the Tevatron and will later be continued at the LHC. Due to the large number of free parameters, a complete scan of the MSSM parameter space is too involved. Therefore at LEP the search has been performed

in three benchmark scenarios [9]. Besides the m_h^{max} scenario, which has been used to obtain conservative bounds on $\tan\beta$ [10], and the no-mixing scenario, the large-μ scenario had been designed to encourage the inclusion of flavor and decay-mode independent decay channels (instead of focusing on the $h \to b\bar{b}$ channel) into the LEP wide combinations. The inclusion of these channels has lead to exclusion bounds [11] that finally completely ruled out the large-μ scenario.

The different environment at hadron colliders implies different Higgs boson production channels and also different relevant decay channels as compared to LEP. The main production modes at the Tevatron will be $V^* \to V\phi$ ($V = W, Z, \phi = h, H$) and also $b\bar{b} \to b\bar{b}\phi$ ($\phi = h, H, A$) while the relevant decay mode will be $\phi \to b\bar{b}$ [12][2]. At the LHC, on the other hand, the most relevant processes for a Higgs boson with $m_h \leq 135\,\mathrm{GeV}$ will be $gg \to h \to \gamma\gamma$ and $t\bar{t} \to t\bar{t}\, h \to t\bar{t}\, b\bar{b}$ [13]. Also the W boson fusion channel, $WW \to h \to \tau^+\tau^-$ has been shown to be promising [14]. In order to investigate these different modes, we propose new benchmark scenarios for the Higgs boson searches at hadron colliders. Contrary to the new "SPS" (Snowmass Points and Slopes) benchmark scenarios proposed in [15] for general supersymmetry (SUSY) searches, the scenarios proposed here are designed specifically to study the MSSM Higgs sector without assuming any particular soft SUSY-

---

[1] This value holds for $m_t = 175\,\mathrm{GeV}$ and $M_{\mathrm{SUSY}} = 1\,\mathrm{TeV}$. If m_t is raised by $5\,\mathrm{GeV}$ then the m_h limit is increased by about $5\,\mathrm{GeV}$; using $M_{\mathrm{SUSY}} = 2\,\mathrm{TeV}$ increases the limit by about $2\,\mathrm{GeV}$

[2] The decay channel $\phi \to \tau^+\tau^-$ at the Tevatron still needs further investigation

breaking scenario and taking into account constraints only from the Higgs boson sector itself (i.e. we do not consider constraints coming from cold dark matter, BR($b \to s\gamma$) or $g_\mu - 2$, which depend on other parameters of the theory, not relevant for Higgs boson physics, or which can easily be avoided; see Sect. 2.1).

The tree-level value for m_h within the MSSM is determined by $\tan\beta$, the $\mathcal{CP}$-odd Higgs boson mass, M_A, and the Z boson mass, M_Z. Beyond the tree level, the main correction to m_h stems from the $t/\tilde{t}$ sector, and for large values of $\tan\beta$ also from the $b/\tilde{b}$ sector (see [9] for our notations). Accordingly, the most important parameters for the corrections to m_h are m_t, M_{SUSY} (in this work we assume that the soft SUSY-breaking parameters for sfermions are equal: $M_{\mathrm{SUSY}} := M_{\tilde{t}_L} = M_{\tilde{t}_R} = M_{\tilde{b}_L} = M_{\tilde{b}_R}$), X_t ($\equiv A_t - \mu/\tan\beta$), and X_b ($\equiv A_b - \mu\tan\beta$); $A_{t,b}$ are the trilinear Higgs sfermion couplings and μ is the Higgs mixing parameter. The mass of the lightest $\mathcal{CP}$-even Higgs boson, m_h, depends furthermore on the SU(2) gaugino mass parameter, M_2 (we assume that the U(1) gaugino mass parameter is given by the GUT relation $M_1 = 5/3\, s_W^2/c_W^2\, M_2$). At the two-loop level also the gluino mass, $m_{\tilde{g}}$, enters the prediction for m_h.

It should be noted in this context that the FD result has been obtained in the on-shell (OS) renormalization scheme (the corresponding Fortran code, that has been used for the analyses by the LEP collaborations, is Feyn-Higgs [16,17]), whereas the RG result has been calculated using the $\overline{\mathrm{MS}}$ scheme; see [18] for details (the corresponding Fortran code, also used by the LEP collaborations, is subhpole [2,3,18]). While the corresponding shift in the parameter M_{SUSY} turns out to be relatively small in general, sizable differences can occur between the numerical values of X_t in the two renormalization schemes; see [8, 18]. For this reason we specify below different values for X_t within the two approaches.

2 The benchmark scenarios

In this section we define four benchmark scenarios suitable for the MSSM Higgs boson search at hadron colliders. In these scenarios the values of the parameters of the $\tilde{t}$ and $\tilde{b}$ sector as well as the gaugino masses will be fixed, while $\tan\beta$ and M_A are the parameters that are varied according to

$$0.5 \leq \tan\beta \leq 50, \quad M_A \leq 1\,\mathrm{TeV}. \tag{1}$$

It has been checked that the new scenarios fulfill the LEP2 bounds [11] over a wide range of the M_A–$\tan\beta$-plane.

To illustrate the effects arising in the different proposed benchmark scenarios, we have evaluated (using the results presented in [19–22])

$$\frac{[\sigma \times \mathrm{BR}]_{\mathrm{MSSM}}}{[\sigma \times \mathrm{BR}]_{\mathrm{SM}}} \tag{2}$$

for several Higgs production and decay channels for the new benchmark scenarios ($\phi = h, H$):

$$(\mathrm{I}): \ gg \to \phi \to \gamma\gamma,$$

$$(\mathrm{II}): \ t\bar{t} \to t\bar{t}\,\phi \to t\bar{t}\,b\bar{b},$$
$$(\mathrm{III}): \ V^* \to V\,\phi \to b\bar{b} \quad (V = Z, W^\pm),$$
$$(\mathrm{IV}): \ WW \to \phi \to \tau^+\tau^-. \tag{3}$$

Since for low values of M_A the heavy $\mathcal{CP}$-even Higgs boson, H, can have SM-like properties, also the corresponding channels with H have to be taken into account. In the case where $m_H - m_h \leq 10\,\mathrm{GeV}$ the signals of both $\mathcal{CP}$-even Higgs bosons would be visible and, as an approximation, have been added up in our analysis[3]. In all the channels always the Higgs boson with the higher $[\sigma \times \mathrm{BR}]_{\mathrm{MSSM}}/[\sigma \times \mathrm{BR}]_{\mathrm{SM}}$ has been taken into account. However, in channel (I) this has been restricted to $m_H \lesssim 140\,\mathrm{GeV}$, in channel (II) to $m_H \lesssim 130\,\mathrm{GeV}$.

In the corresponding figures shown below, we restrict ourselves to $M_A \leq 500\,\mathrm{GeV}$, since most deviations of the MSSM from the SM occur in this M_A range. While it has been shown that the Higgs sector of the MSSM behaves like the SM Higgs sector if the SUSY mass scales *and* M_A approach infinity (see e.g. [23] for a one-loop analysis, and references therein), we do not find complete decoupling, since the SUSY mass scales are kept fixed.

In the figures presented below, we also mark the region excluded by LEP Higgs boson searches [11]. The Higgs boson masses have been evaluated with the same code as used so far by the LEP Higgs working group. However, most recently obtained corrections [6,17] can yield somewhat higher values for m_h, depending on the scenario. This increase in m_h does not affect the general phenomenological features shown in the plots below. Further information about the effect of the most recently obtained corrections and further plots for the new benchmark scenarios can be found at www.feynhiggs.de.

2.1 The m_h^{max} scenario

This scenario is kept as presented in [9], since it allows conservative $\tan\beta$ exclusion bounds [10] (only the sign of μ is switched to a positive value). The parameters are chosen such that the maximum possible Higgs boson mass as a function of $\tan\beta$ is obtained (for fixed M_{SUSY} and m_t, and M_A set to its maximal value, $M_A = 1\,\mathrm{TeV}$). The parameters are[4]:

$$m_t = 174.3\,\mathrm{GeV},$$
$$M_{\mathrm{SUSY}} = 1\,\mathrm{TeV},$$
$$\mu = 200\,\mathrm{GeV},$$

---

[3] In order to treat this situation more appropriately, additional experimental analyses are necessary

[4] As mentioned above, no external constraints are taken into account. In the minimal flavor violation scenario, better agreement with BR($b \to s\gamma$) constraints would be obtained for the other sign of X_t [24] (called the "constrained m_h^{max}" scenario). But, since this lowers the maximum m_h values by $\sim 5\,\mathrm{GeV}$ and BR($b \to s\gamma$) can be changed drastically by deviating from the minimal flavor violation scenario [25] without affecting the Higgs boson sector phenomenology, the m_h^{max} scenario is defined with positive X_t
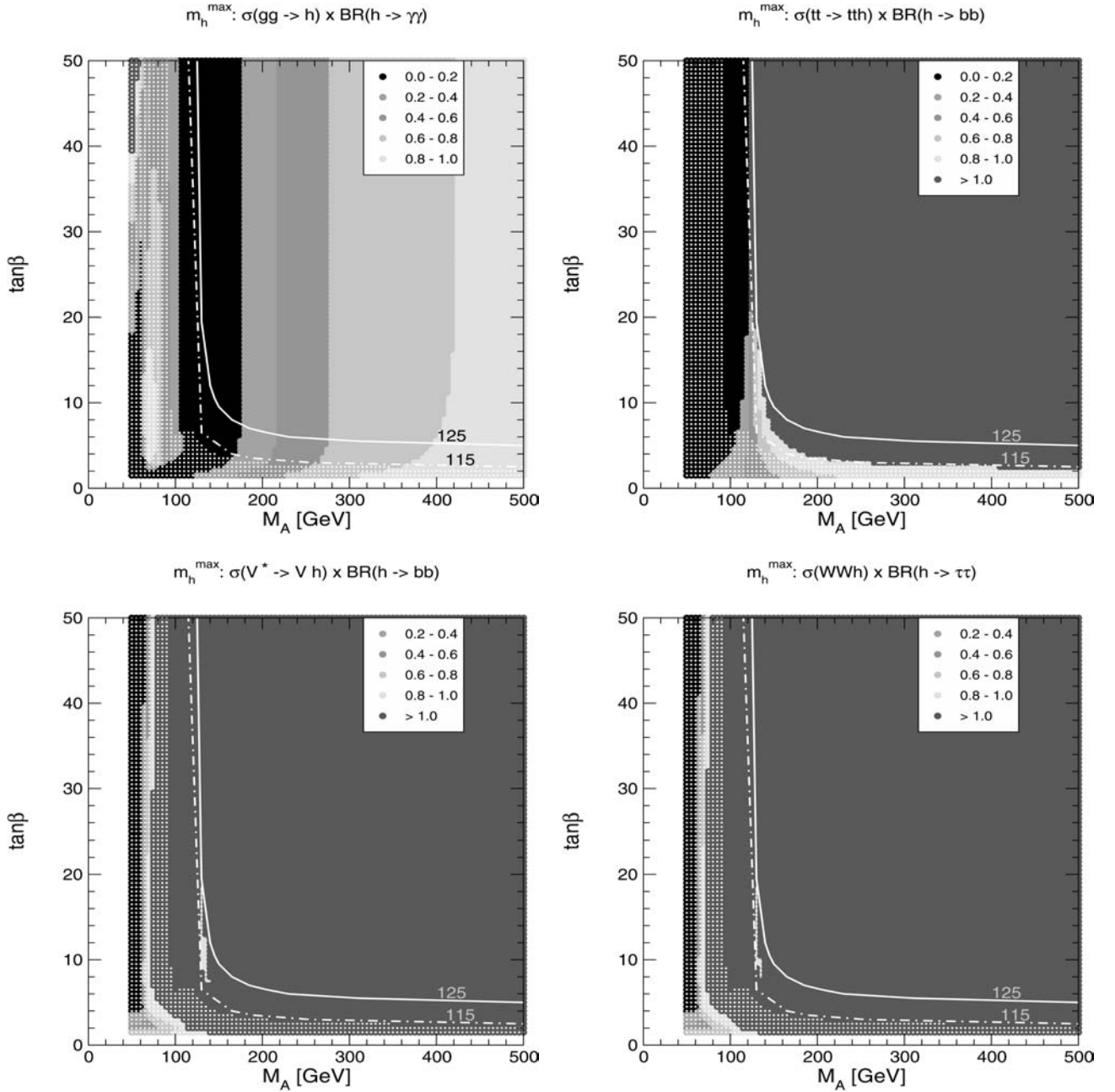
Fig. 1. $[\sigma \times \mathrm{BR}]_{\mathrm{MSSM}}/[\sigma \times \mathrm{BR}]_{\mathrm{SM}}$ is shown for the channels $gg \to h \to \gamma\gamma$ (*upper left plot*), $t\bar{t} \to t\bar{t}\,h \to t\bar{t}\,b\bar{b}$ (*upper right*), $V^* \to Vh \to Vb\bar{b}$ (*lower left*) and $WW \to h \to \tau^+\tau^-$ (*lower left*) in the M_A–$\tan\beta$-plane for the m_h^{max} scenario. The white-dotted area is excluded by LEP Higgs searches. The dot-dashed curve corresponds to $m_h = 115\,\mathrm{GeV}$, the solid curve to $m_h = 125\,\mathrm{GeV}$

$$
\begin{aligned}
M_2 &= 200\,\mathrm{GeV}, \\
X_t^{\mathrm{OS}} &= 2\,M_{\mathrm{SUSY}} \ \ \text{(FD calculation)}, \\
X_t^{\overline{\mathrm{MS}}} &= \sqrt{6}\,M_{\mathrm{SUSY}} \ \ \text{(RG calculation)} \\
A_b &= A_t, \\
m_{\tilde{g}} &= 0.8\,M_{\mathrm{SUSY}}.
\end{aligned} \tag{4}
$$

In Fig. 1 we show $[\sigma \times \mathrm{BR}]_{\mathrm{MSSM}}/[\sigma \times \mathrm{BR}]_{\mathrm{SM}}$ for the channels $gg \to h \to \gamma\gamma$ (upper left plot) and $t\bar{t} \to t\bar{t}\,h \to t\bar{t}\,b\bar{b}$ (upper right), $W^* \to Wh \to Wb\bar{b}$ (lower left) and $WW \to h \to \tau^+\tau^-$ (lower left) in the M_A–$\tan\beta$-plane.

For low values of the $\mathcal{CP}$-odd Higgs boson mass, M_A, the structure of the MSSM Higgs sector leads to an enhancement of the $hb\bar{b}$ and $h\tau^+\tau^-$ couplings with respect to the SM value. In the MSSM these couplings possess an additional factor of $-\sin\alpha_{\mathrm{eff}}/\cos\beta$, where α_{eff} is the mixing angle of the neutral $\mathcal{CP}$-even Higgs sector, including radiative corrections (see e.g. [21,22]; in this case the genuine vertex corrections are small). The factor of $1/\cos\beta$ can lead to an enhancement for large $\tan\beta$. The factor $-\sin\alpha_{\mathrm{eff}}/\cos\beta$ in the couplings converges very slowly to 1 for large values of M_A, and can differ significantly for low
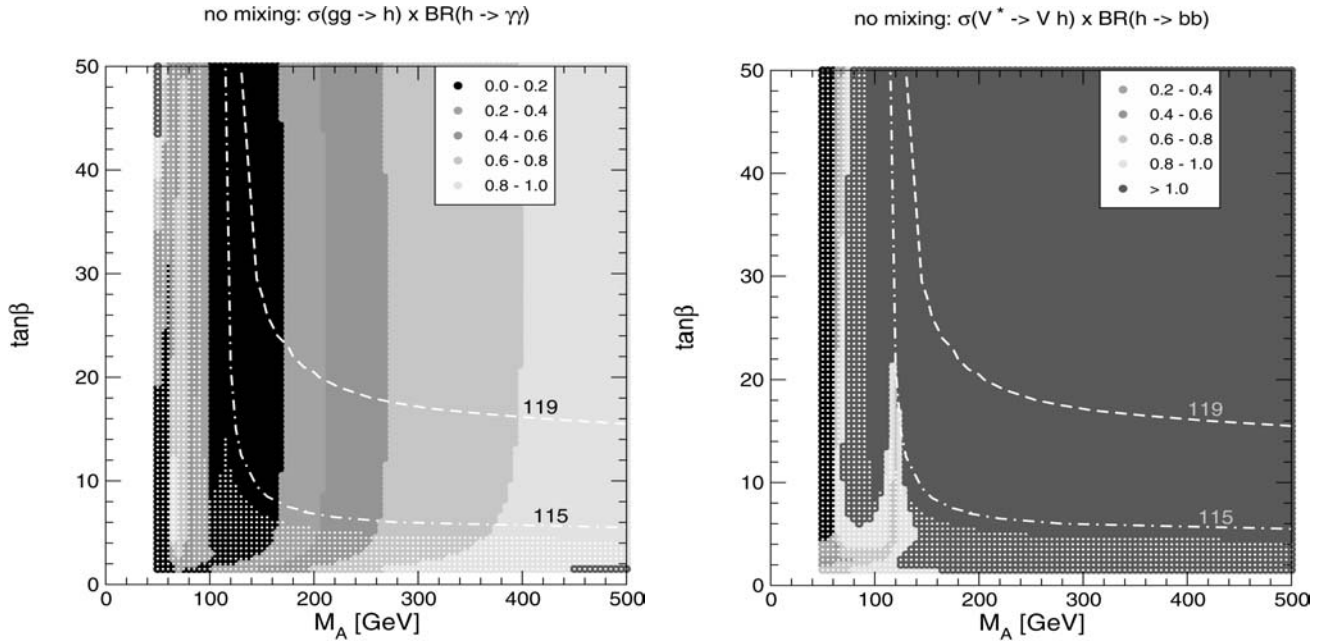
Fig. 2. $[\sigma \times \mathrm{BR}]_{\mathrm{MSSM}}/[\sigma \times \mathrm{BR}]_{\mathrm{SM}}$ is shown for the channels $gg \to h \to \gamma\gamma$ (*left plot*) and $V^* \to Vh \to Vb\bar{b}$ (*right plot*) in the M_A–$\tan\beta$-plane for the no-mixing scenario. The white-dotted area is excluded by LEP Higgs searches. The dot-dashed curve corresponds to $m_h = 115\,\mathrm{GeV}$, the short-dashed curve to $m_h = 119\,\mathrm{GeV}$

values of M_A. In the case of strong enhancement of $h \to b\bar{b}$ and $h \to \tau^+\tau^-$, the branching ratio of the decay of h into other particles, in particular the $h \to \gamma\gamma$ channel, is significantly suppressed. Therefore, the $gg \to h \to \gamma\gamma$ channel can be strongly suppressed for small and moderate values of M_A. The $W^* \to Wh \to Wb\bar{b}$ channel, on the other hand, is nearly always enhanced compared to the SM case, since the WWh coupling is mostly SM-like, except for $M_A \lesssim 100\,\mathrm{GeV}$, where for intermediate and large values of $\tan\beta$ the WWh coupling becomes small. In this parameter region, however, for very small values of M_A the heavy $\mathcal{CP}$-even Higgs boson, H, has SM-like couplings. As a consequence, in the parameter regions where the light Higgs boson is very difficult to observe, the search for the H should have similar prospects as the SM Higgs search. This results in an enhanced value of $[\sigma \times \mathrm{BR}]_{\mathrm{MSSM}}/[\sigma \times \mathrm{BR}]_{\mathrm{SM}}$ also for $M_A \lesssim 100\,\mathrm{GeV}$.

The four entries in Fig. 1 show the complementarity for the four channels between Tevatron and LHC for the search for the lightest MSSM Higgs boson.

2.2 The no-mixing scenario

This benchmark scenario is associated with vanishing mixing in the $\tilde{t}$ sector and with a higher SUSY mass scale as compared to the $m_h^{\max}$ scenario to increase the parameter space that avoids the LEP Higgs bounds:

$$m_t = 174.3\,\mathrm{GeV},$$
$$M_{\mathrm{SUSY}} = 2\,\mathrm{TeV},$$
$$\mu = 200\,\mathrm{GeV},$$
$$M_2 = 200\,\mathrm{GeV},$$

$$X_t = 0 \text{ (FD/RG calculation)},$$
$$A_b = A_t,$$
$$m_{\tilde{g}} = 0.8\,M_{\mathrm{SUSY}}. \tag{5}$$

In Fig. 2 we show $[\sigma \times \mathrm{BR}]_{\mathrm{MSSM}}/[\sigma \times \mathrm{BR}]_{\mathrm{SM}}$ for the channels $gg \to h \to \gamma\gamma$ (left plot) and $W^* \to Wh \to Wb\bar{b}$ (right plot) in the M_A–$\tan\beta$-plane. As in the $m_h^{\max}$ scenario, the branching ratio for $h \to b\bar{b}$ and $h \to \tau^+\tau^-$ is significantly enhanced for low values of M_A. Therefore, also in the no-mixing scenario the $gg \to h \to \gamma\gamma$ channel can be strongly suppressed for not too large values of M_A. The $W^* \to Wh \to Wb\bar{b}$ channel is nearly always enhanced compared to the SM case for the same reasons as in the $m_h^{\max}$ scenario. This holds except for $M_A \lesssim 100\,\mathrm{GeV}$, where the channel $W^* \to WH \to Wb\bar{b}$ takes over and results in an enhanced value of $[\sigma \times \mathrm{BR}]_{\mathrm{MSSM}}/[\sigma \times \mathrm{BR}]_{\mathrm{SM}}$ for the heavy $\mathcal{CP}$-even Higgs boson.

2.3 The gluophobic Higgs scenario

In this scenario the main production cross section for the light Higgs boson at the LHC, $gg \to h$, is strongly suppressed for a wide range of the M_A–$\tan\beta$-plane. This happens due to a cancellation between the top quark and the stop quark loops in the production vertex (see [26]). This cancellation is more effective for small $\tilde{t}$ masses (in agreement with the exclusion bounds for $\tilde{t}$ masses from LEP and the Tevatron [27]) and for relatively large values of the $\tilde{t}$ mixing parameter, X_t. The partial width of the most relevant decay mode, $\Gamma(h \to \gamma\gamma)$, is affected much less, since it is dominated by the W boson loop. The parameters are
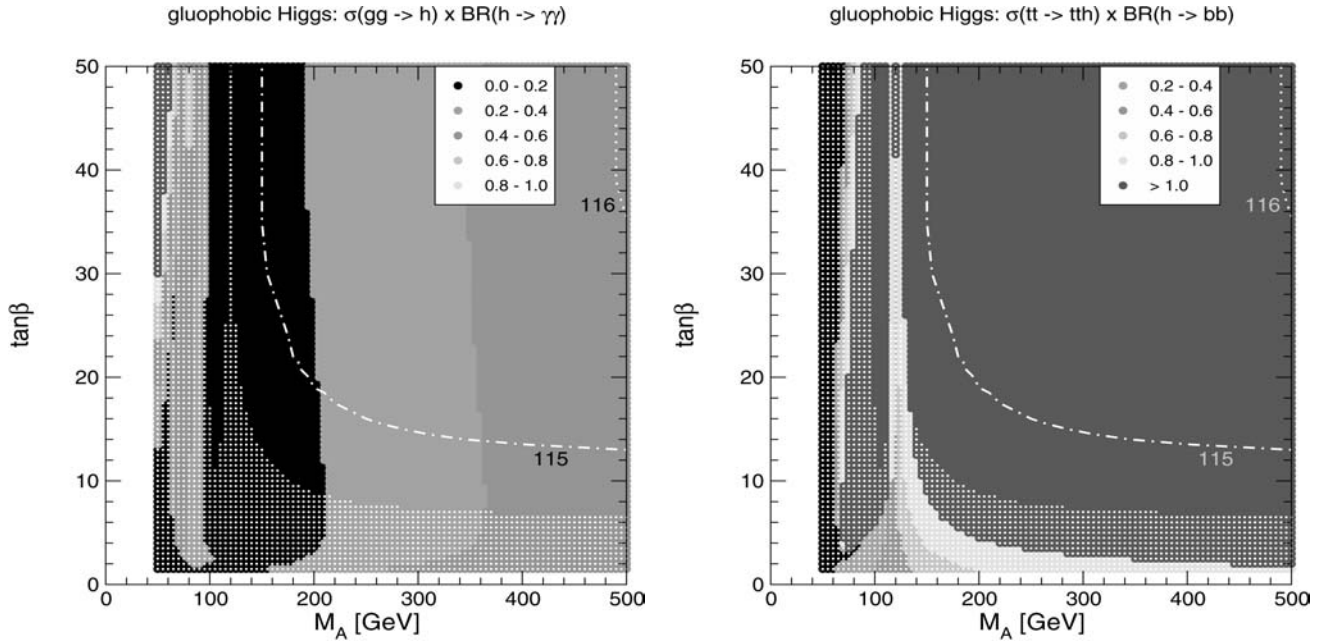
Fig. 3. $[\sigma \times \mathrm{BR}]_{\mathrm{MSSM}}/[\sigma \times \mathrm{BR}]_{\mathrm{SM}}$ is shown for the channels $gg \to h \to \gamma\gamma$ (*left plot*) and $t\bar{t} \to t\bar{t}h \to t\bar{t}b\bar{b}$ (*right plot*) in the M_A–$\tan\beta$-plane for the gluophobic Higgs scenario. The white-dotted area is excluded by LEP Higgs searches. The dot-dashed curve corresponds to $m_h = 115\,\mathrm{GeV}$, the dotted curve to $m_h = 116\,\mathrm{GeV}$

$$m_t = 174.3\,\mathrm{GeV},$$
$$M_{\mathrm{SUSY}} = 350\,\mathrm{GeV},$$
$$\mu = 300\,\mathrm{GeV},$$
$$M_2 = 300\,\mathrm{GeV},$$
$$X_t^{\mathrm{OS}} = -750\,\mathrm{GeV}\ (\text{FD calculation}),$$
$$X_t^{\overline{\mathrm{MS}}} = -770\,\mathrm{GeV}\ (\text{RG calculation})$$
$$A_b = A_t,$$
$$m_{\tilde{g}} = 500\,\mathrm{GeV}. \tag{6}$$

In Fig. 3 we show $[\sigma \times \mathrm{BR}]_{\mathrm{MSSM}}/[\sigma \times \mathrm{BR}]_{\mathrm{SM}}$ for the channels $gg \to h \to \gamma\gamma$ (left plot) and $t\bar{t} \to t\bar{t}\,h \to t\bar{t}\,b\bar{b}$ (right plot) in the M_A–$\tan\beta$-plane. The $gg \to h \to \gamma\gamma$ channel can be strongly suppressed over the whole M_A–$\tan\beta$-plane (even for $M_A = 1000\,\mathrm{GeV}$ a suppression of about 50% takes place), rendering this detection channel difficult. The $t\bar{t} \to t\bar{t}\,h \to t\bar{t}\,b\bar{b}$ channel, on the other hand, is always enhanced compared to the SM case. This holds except for $M_A \lesssim 100\,\mathrm{GeV}$, where again the detection of H takes over. The same qualitative behavior holds for the WW fusion channel with subsequent decay to $b\bar{b}$ or $\tau^+\tau^-$.

2.4 The small α_{eff} scenario

Besides the channel $gg \to h \to \gamma\gamma$ at the LHC, the other channels for light Higgs searches at the Tevatron and at the LHC mostly rely on the decays $h \to b\bar{b}$ and $h \to \tau^+\tau^-$; see Sect. 2.1. If α_{eff} is small, these two decay channels can be heavily suppressed in the MSSM due to the additional factor $-\sin\alpha_{\mathrm{eff}}/\cos\beta$ compared to the SM coupling. The

decay $h \to b\bar{b}$ can also be affected by large vertex corrections from $\tilde{b}$–$\tilde{g}$ loops [20,21]. These vertex corrections can change the basic relation $g_{hb\bar{b}}/g_{h\tau^+\tau^-} = m_b/m_\tau$, resulting in different regions of suppression for both decay channels. Such a suppression occurs for large $\tan\beta$ and not too large M_A (in a similar way as in the large-μ scenario [9]) for the following parameters:

$$m_t = 174.3\,\mathrm{GeV},$$
$$M_{\mathrm{SUSY}} = 800\,\mathrm{GeV},$$
$$\mu = 2.5\,M_{\mathrm{SUSY}},$$
$$M_2 = 500\,\mathrm{GeV},$$
$$X_t^{\mathrm{OS}} = -1100\,\mathrm{GeV}\ (\text{FD calculation}),$$
$$X_t^{\overline{\mathrm{MS}}} = -1200\,\mathrm{GeV}\ (\text{RG calculation})$$
$$A_b = A_t,$$
$$m_{\tilde{g}} = 500\,\mathrm{GeV}. \tag{7}$$

In Fig. 4 we show $[\sigma \times \mathrm{BR}]_{\mathrm{MSSM}}/[\sigma \times \mathrm{BR}]_{\mathrm{SM}}$ for the channels $gg \to h \to \gamma\gamma$ (upper plot) $W^* \to Wh \to Wb\bar{b}$ (lower left) and $WW \to h \to \tau^+\tau^-$ (lower right) in the M_A–$\tan\beta$-plane. Significant suppression occurs for the latter two channels for large $\tan\beta$, $\tan\beta \gtrsim 20$, and small M_A, $M_A \lesssim 250, 300\,\mathrm{GeV}$, for $h \to b\bar{b}$ and $h \to \tau^+\tau^-$, respectively. Thus, Higgs boson search via the W production channel and the WW fusion channel (see also [14]) will be difficult in these parts of the parameter space. The same applies for the channel $t\bar{t}h \to t\bar{t}b\bar{b}$ (which is not shown here). The complementary channel, $h \to \gamma\gamma$, is enhanced compared to the SM case in the parts of the M_A–$\tan\beta$-plane where the channels (III) and (IV) are suppressed.
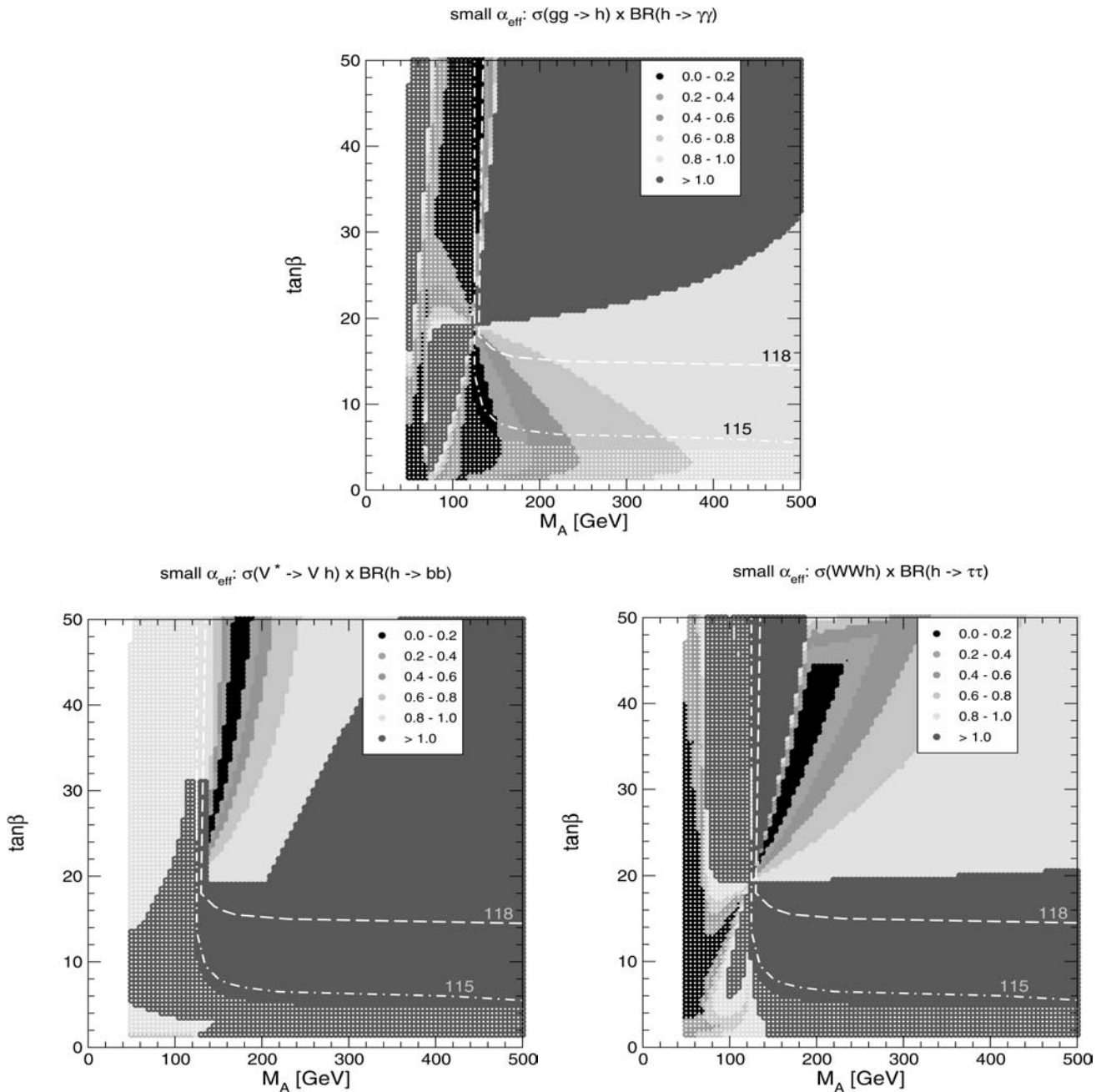
small α_{eff}: $\sigma(gg \rightarrow h) \times BR(h \rightarrow \gamma\gamma)$

small α_{eff}: $\sigma(V^* \rightarrow V h) \times BR(h \rightarrow bb)$

small α_{eff}: $\sigma(WWh) \times BR(h \rightarrow \tau\tau)$

Fig. 4. $[\sigma \times BR]_{\text{MSSM}}/[\sigma \times BR]_{\text{SM}}$ is shown for the channels $gg \rightarrow h \rightarrow \gamma\gamma$ (*upper plot*) $W^* \rightarrow Wh \rightarrow Wb\bar{b}$ (*lower left*) and $W^* \rightarrow Wh \rightarrow W\tau^+\tau^-$ (*lower right*) in the M_A–$\tan\beta$-plane for the small α_{eff} scenario. The white-dotted area is excluded by LEP Higgs searches. The dot-dashed curve corresponds to $m_h = 115\,\text{GeV}$, the long-dashed curve to $m_h = 118\,\text{GeV}$

3 Conclusions

We have proposed four benchmark scenarios for the MSSM Higgs boson search at hadron colliders, which take into account the exclusion bounds obtained at LEP2. The different scenarios exemplify different features of the MSSM parameter space, such as large m_h values and significant $gg \rightarrow h$ or $h \rightarrow b\bar{b}$, $h \rightarrow \tau^+\tau^-$ suppression. In the benchmark scenarios proposed above, we have briefly analyzed the possible suppression of several Higgs produc-

tion and decay channels, showing possible "problematic" regions of the MSSM parameter space.

With the exception of the gluon fusion mediated production process, which is significantly suppressed in the gluophobic Higgs scenario, the production processes at the Tevatron and the LHC considered here, $V^* \rightarrow Vh$, $t\bar{t} \rightarrow t\bar{t}\,h$, $WW \rightarrow h$ and $gg \rightarrow h$, are close to their SM values for most of the allowed parameter space of the benchmark scenarios. (For small values of M_A this behavior can be observed for the heavy $\mathcal{CP}$-even Higgs boson.)

Hence, deviations of the rate of the Higgs search processes at hadron colliders compared to the SM case are mainly due to the SUSY corrections affecting the Higgs decay modes.

In all the cases analyzed in this note, we have found a complementarity between the $h \to b\bar{b}$, $h \to \tau^+\tau^-$ and the $h \to \gamma\gamma$ channels, i.e. in the parameter regions where the search for the Higgs in one of these channels becomes problematic, in at least one of the other channels it becomes easier than in the SM case. It is difficult to find exceptions to this rule in the MSSM parameter space. Therefore in analyzing the new benchmark scenarios, it will be helpful to make use of the complementarity of different channels accessible at the Tevatron and the LHC (see e.g. [21] for details).

References

1. H. Haber, R. Hempfling, Phys. Rev. Lett. **66**, 1815 (1991); Y. Okada, M. Yamaguchi, T. Yanagida, Prog. Theor. Phys. **85**, 1 (1991); J. Ellis, G. Ridolfi, F. Zwirner, Phys. Lett. B **257**, 83 (1991); Phys. Lett. B **262**, 477 (1991); R. Barbieri, M. Frigeni, Phys. Lett. B **258**, 395 (1991); P. Chankowski, S. Pokorski, J. Rosiek, Phys. Lett. B **274**, 191 (1992); A. Dabelstein, Z. Phys. C **67**, 495 (1995), hep-ph/9409375

2. M. Carena, J. Espinosa, M. Quirós, C. Wagner, Phys. Lett. B **355**, 209 (1995), hep-ph/9504316

3. M. Carena, M. Quirós, C. Wagner, Nucl. Phys. B **461**, 407 (1996), hep-ph/9508343, see fnth37.fnal.gov/carena/

4. H. Haber, R. Hempfling, A. Hoang, Z. Phys. C **75**, 539 (1997), hep-ph/9609331

5. R.-J. Zhang, Phys. Lett. B **447**, 89 (1999), hep-ph/9808299; J. Espinosa, R.-J. Zhang, Nucl. Phys. B **586**, 3 (2000), hep-ph/0003246

6. A. Brignole, G. Degrassi, P. Slavich, F. Zwirner, Nucl. Phys. B **631**, 195 (2002), hep-ph/0112177; hep-ph/0206101

7. S. Heinemeyer, W. Hollik, G. Weiglein, Phys. Rev. D **58**, 091701 (1998), hep-ph/9803277; Phys. Lett. B **440**, 296 (1998), hep-ph/9807423

8. S. Heinemeyer, W. Hollik, G. Weiglein, Eur. Phys. J. C **9**, 343 (1999), hep-ph/9812472

9. M. Carena, S. Heinemeyer, C. Wagner, G. Weiglein, hep-ph/9912223

10. S. Heinemeyer, W. Hollik, G. Weiglein, JHEP **0006**, 009 (2000), hep-ph/9909540

11. LEP Higgs Working Group Collaboration, hep-ex/0107030

12. M. Carena et al., Report of the Tevatron Higgs working group, hep-ph/0010338

13. ATLAS Collaboration, Detector and Physics Performance Technical Design Report, CERN/LHCC/99-15 (1999); see atlasinfo.cern.ch/Atlas/GROUPS/PHYSICS/TDR/access.html

14. T. Plehn, D. Rainwater, D. Zeppenfeld, Phys. Lett. B **454**, 297 (1999), hep-ph/9902434

15. B. Allanach et al., The Snowmass Points and Slopes: Benchmarks for SUSY Searches, to appear in the Proceedings of the Workshop on the Future of High Energy Physics, Snowmass, July 2001, hep-ph/0202233

16. S. Heinemeyer, W. Hollik, G. Weiglein, Comp. Phys. Comm. **124**, 76 (2000), hep-ph/9812320; hep-ph/0002213; see www.feynhiggs.de

17. M. Frank, S. Heinemeyer, W. Hollik, G. Weiglein, hep-ph/0202166

18. M. Carena, H. Haber, S. Heinemeyer, W. Hollik, C. Wagner, G. Weiglein, Nucl. Phys. B **580**, 29 (2000), hep-ph/0001002

19. A. Djouadi, J. Kalinowski, M. Spira, Comp. Phys. Comm. **108**, 56 (1998), hep-ph/9704448

20. R. Hempfling, Phys. Rev. D **49**, 6168 (1994); L.J. Hall, R. Rattazzi, U. Sarid, Phys. Rev. D **50**, 7048 (1994), hep-ph/9306309; M. Carena, M. Olechowski, S. Pokorski, C. Wagner, Nucl. Phys. B **426**, 269 (1994), hep-ph/9402253

21. M. Carena, S. Mrenna, C. Wagner, Phys. Rev. D **60**, 075010 (1999), hep-ph/9808312; Phys. Rev. D **62**, 055008 (2000), hep-ph/9907422

22. S. Heinemeyer, W. Hollik, G. Weiglein, Eur. Phys. J. C **16**, 139 (2000), hep-ph/0003022

23. H. Haber, M. Herrero, H. Logan, S. Peñaranda, S. Rigolin, D. Temes, Phys. Rev. D **63**, 055004 (2001), hep-ph/0007006

24. G. Degrassi, P. Gambino, G. Giudice, JHEP **0012**, 009 (2000), hep-ph/0009337; M. Carena, D. Garcia, U. Nierste, C. Wagner, Phys. Lett. B **499**, 141 (2001), hep-ph/0010003

25. F. Gabbiani, E. Gabrielli, A. Masiero, L. Silvestrini, Nucl. Phys. B **477**, 321 (1996), hep-ph/9604387; F. Borzumati, C. Greub, T. Hurth, D. Wyler, Phys. Rev. D **62**, 075005 (2000), hep-ph/9911245

26. A. Djouadi, Phys. Lett. B **435**, 101 (1998), hep-ph/9806315

27. Part. Data Group, Eur. Phys. J. C **15**, 1 (2000)